



# Multi-flexural band gaps in an Euler–Bernoulli beam with lateral local resonators



Ting Wang<sup>a,b</sup>, Mei-Ping Sheng<sup>a</sup>, Qing-Hua Qin<sup>b</sup>

<sup>a</sup> School of Marine Science and Technology, Northwestern Polytechnical University, Xi'an, Shaanxi, 710072, PR China

<sup>b</sup> College of Engineering and Computer Science, The Australian National University, ACT, 2600, Australia

## ARTICLE INFO

### Article history:

Received 30 September 2015

Received in revised form 1 December 2015

Accepted 2 December 2015

Available online 10 December 2015

Communicated by R. Wu

### Keywords:

Flexural vibration suppression

Lateral local resonator

Band gaps

Wave transformation

Frequency response function

## ABSTRACT

Flexural vibration suppression in an Euler–Bernoulli beam with attached lateral local resonators (LLR) is studied theoretically and numerically. Hamilton's principle and Bloch's theorem are employed to derive the dispersion relation which reveals that two band gaps are generated. Within both band gaps, the flexural waves are partially transformed into longitudinal waves through a four-link-mechanism and totally blocked. The band gaps can be flexibly tuned by changing the geometry parameter of the four-link-mechanism and the spring constants of the resonators. Frequency response function (FRF) from finite element analysis via commercial software of ANSYS shows large flexural wave attenuation within the band gaps and the effect of damping from the LLR substructures which helps smooth and lower the response peaks at the sacrifice of the band gap effect. The existence of the multi-flexural band gaps can be exploited for the design of flexural vibration control of beams.

© 2015 Elsevier B.V. All rights reserved.

## 1. Introduction

Investigations on wave propagation in periodic structures have received much attention in recent years [1–4]. The studies are focused on the generating of unique band gaps within which acoustic waves are totally attenuated. Their related applications are promising in vibration isolators, frequency filters and waveguides. Previous configurations proposed in Refs. [5–7] are mainly on one-dimensional lattice for controlling the longitudinal wave behaviour, which is far from practical application.

Beams are widely used in engineering constructions. Waves propagating through beams may cause damages for the structures and inaccuracy for some experimental measurements. Several structural configurations using the band gap concept have been designed for the control of the behaviour of waves in beams. In the configurations, the local resonators are attached to continuum beams to generate band gaps for stopping the propagation of waves, including longitudinal wave [8], flexural wave [9–11] and torsional wave [12]. As for practical engineering applications, the control of flexural wave is of great importance for structures working under water regarding their radiation safety. With this awareness, Yu et al. [13] and Liu et al. [14] investigated flexural wave in different types of beams to prevent its propagation, which provides guidance in vibration suppression design.

Sun et al. [15] attached small spring–mass–damper subsystems to a uniform isotropic beam to form a metamaterial, aiming at band gap generation for flexural vibration absorption.

Beams mentioned above yield only single band gap, which is inapplicable to devices or cases requiring multi-flexural wave suppression. Besides, design and modelling of beams having multi-flexural band gaps is more difficult due to their higher DOFs. Few researches have been carried out on this. So far, Wen et al. [16] and Wang et al. [17] designed a multi-band gap beam by attaching multi-local resonators periodically to a beam based on previous single band gap concept. Their work paved a way for multi-wave suppression. Pai later extended their previous work [18], developing modelling and analysis methods to reveal the actual working mechanism of the multi-band gaps metamaterial beam for absorption of low frequency waves. All the work they've done focuses on the attachment of multi-resonators for the flexural wave control. No one has transformed the flexural waves to longitudinal waves and attenuated the flexural vibration in another direction in a beam.

Inspired by the LLR configuration proposed by Huang and Sun [19], this paper proposes a new metamaterial beam to generate multi-flexural band gaps with LLR substructures attached. The LLR structures can partially transform the flexural waves into longitudinal waves, and block the wave propagation in another direction. The rest of this letter is organised as follows. A concise derivation of the Hamilton's principles of the LLR beam is provided in Section 2 and validated using the finite element method in Section 3

E-mail address: WT323@mail.nwpu.edu.cn (T. Wang).

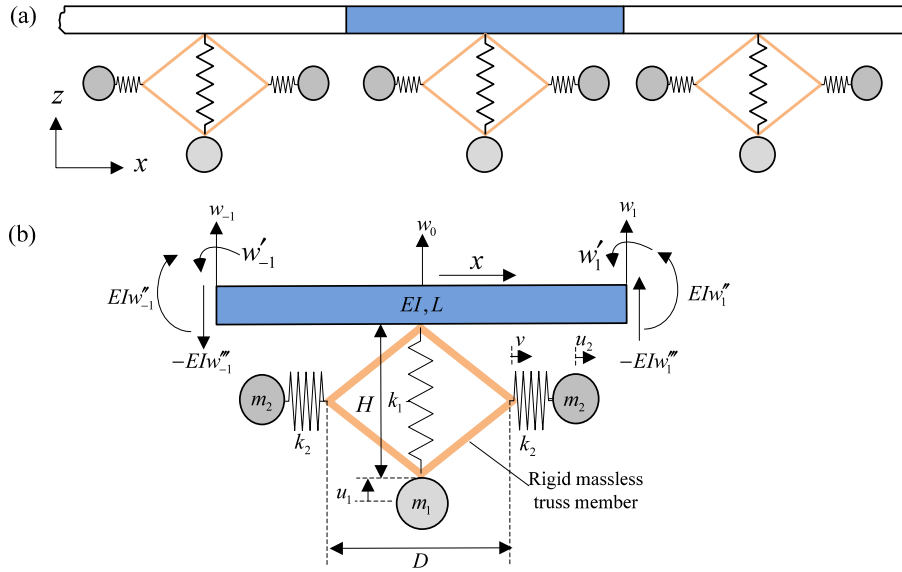


Fig. 1. Construction of metamaterial beam: (a) an infinite beam, (b) a typical unit cell.

[20], with the analysis of the effect of the geometry parameters and damping on the band gaps. Design of the multi-band gap beams in applications is presented in the section of conclusion.

## 2. Theory and modelling

Fig. 1 shows a simple model of an Euler–Bernoulli beam with periodical LLR substructures in  $x$  direction. One LLR consists of two lateral resonators with spring and mass constant of  $k_2$  and  $m_2$ , a vertical resonator with spring and mass constant of  $k_1$  and  $m_1$ , and a four-link-mechanism with rigid and massless trusses. The beam and the vertical resonator vibrate in  $z$  direction and the lateral resonators vibrate in  $x$  directions, with displacements of  $w$ ,  $u_1$  and  $u_2$ , respectively. The vertical distance and the horizontal distance of the four-link-mechanism are  $H$  and  $D$ . The length of the unit cell is  $L$ , and  $A$ ,  $I$ ,  $E$  and  $\rho$  denote the beam's cross-section area, area moment, Young's modulus and mass density, respectively. The dispersion relation is derived below.

The governing equation for a unit cell of an infinite periodic metamaterial beam can be obtained by using the extended Hamilton's principle

$$\int_0^L (\delta T - \delta U + \delta W_{nc}) dt = 0 \quad (1)$$

where  $K$  is the kinetic energy,  $U$  is the elastic energy, and  $W_{nc}$  is the non-conservative work from the external loads. From the typical unit cell, every item in Eq. (1) follows

$$\delta T = - \int_{-L/2}^{L/2} \rho A \dot{w} \dot{w} dx - m_1 \dot{u}_1 \delta u_1 - 2m_2 \dot{u}_2 \delta u_2 \quad (2)$$

$$\begin{aligned} \delta U &= \int_{-L/2}^{L/2} EI w'' \delta w'' dx + k_1 (u_1 - w_0) \delta (u_1 - w_0) \\ &\quad + 2k_2 (u_2 - v) \delta (u_2 - v) \\ &= \int_{-L/2}^{L/2} EI w^{(4)} \delta w dx + k_1 (u_1 - w_0) \delta (u_1 - w_0) \end{aligned}$$

$$\begin{aligned} &+ 2k_2 (u_2 - v) \delta (u_2 - v) \\ &+ EI (w_1'' \delta w_1' - w_{-1}'' \delta w_{-1}' - w_1''' \delta w_1 \\ &+ w_0''' \delta w_0 - w_0''' \delta w_0 + w_{-1}''' \delta w_{-1}) \end{aligned} \quad (3)$$

$$\delta W_{nc} = EI w_1'' \delta w_1' - EI w_{-1}'' \delta w_{-1}' + EI w_{-1}''' \delta w_{-1} - EI w_1''' \delta w_1 \quad (4)$$

Based on the assumption of small displacements, we have

$$v = -\frac{H}{2D} (w_0 - u_1) \quad (5)$$

where  $w_0$  represents the flexural displacement of the centre of the beam, and  $v$  is the displacement of the truss end connected the lateral resonators. Substitution Eqs. (2)–(5) into Eq. (1) yields

$$\begin{aligned} 0 &= \int_0^t \left\{ \int_{-L/2}^{L/2} \left[ -\rho A \ddot{w} - EI w^{(4)} \right. \right. \\ &\quad + \left[ k_1 (u_1 - w_0) - \frac{H}{D} k_2 \left( u_2 + \frac{H}{2D} (w_0 - u_1) \right) \right. \\ &\quad + \left. \left. EI (w_0''' \delta w_0 - w_0''' \delta w_0) \right] \delta(x) \right\} \delta w dx \\ &\quad + \left[ -m_1 \ddot{u}_1 - k_1 (u_1 - w_0) \right. \\ &\quad + \left. \frac{H}{D} k_2 \left( u_2 + \frac{H}{2D} (w_0 - u_1) \right) \right] \delta u_1 \\ &\quad + \left[ -2m_2 \ddot{u}_2 - 2k_2 \left( u_2 + \frac{H}{2D} (w_0 - u_1) \right) \right] \delta u_2 \Big\} dt \end{aligned} \quad (6)$$

where  $\delta(x)$  is the Dirac function,  $w' = \partial w / \partial x$  and  $\dot{w} = \partial w / \partial t$ . Moreover,  $EI w_0''' \neq EI w_0'''$  because of a concentrated shear force created by the LLR substructure at  $x = 0$ . By setting the coefficients of  $\delta w$ ,  $\delta u_1$  and  $\delta u_2$  in Eq. (6) to zero, the governing equations can be obtained.

$$-\rho A \ddot{w} - EI w^{(4)} + \left[ k_1 (u_1 - w_0) - \frac{H}{D} k_2 \left( u_2 + \frac{H}{2D} (w_0 - u_1) \right) \right]$$

$$+ EI(w_{0+}''''\delta w_0 - w_{0-}''''\delta w_0) \Big] \delta(x) = 0 \quad (7)$$

$$-m_1\ddot{u}_1 - k_1(u_1 - w_0) + \frac{H}{D}k_2\left(u_2 + \frac{H}{2D}(w_0 - u_1)\right) = 0 \quad (8)$$

$$-2m_2\ddot{u}_2 - 2k_2\left(u_2 + \frac{H}{2D}(w_0 - u_1)\right) = 0 \quad (9)$$

Due to the periodicity along  $x$  direction, based on the Bloch's theorem, flexural wave propagating through the infinite periodic beam can be expressed in a harmonic form.

$$w(x, t) = We^{j(\beta x - \omega t)}, \quad w_0(t) = W_0e^{-j\omega t}, \\ u_1(t) = U_1e^{-j\omega t}, \quad u_2(t) = U_2e^{-j\omega t} \quad (10)$$

where  $\beta$  and  $\omega$  are the wave number and vibration frequency, respectively. The phase velocity of the flexural wave in this beam is  $c_p = \omega/\beta$ .

If the metamaterial beam is treated as a homogenized uniform beam, Eq. (7) can be integrated over the whole unit cell with harmonic wave solutions.

$$-\int_{-L/2}^{L/2} \rho A \ddot{w} dx - EI(w_1'''' - w_{-1}'''' + k_1(u_1 - w_0) - \frac{H}{D}k_2\left(u_2 + \frac{H}{2D}(w_0 - u_1)\right)) = 0 \quad (11)$$

$$\tilde{m}\ddot{w}_0 + \tilde{k}w_0 + k_1(u_1 - w_0) - \frac{H}{D}k_2\left(u_2 + \frac{H}{2D}(w_0 - u_1)\right) = 0 \quad (12)$$

$$\tilde{m} = -\frac{2\rho A \sin(\beta L/2)}{\beta}, \quad \tilde{k} = -2EI\beta^3 \sin(\beta L/2) \quad (13)$$

Combination of Eq. (12) with Eq. (8) and Eq. (9) yields

$$\begin{bmatrix} -\tilde{m}\omega^2 + \tilde{k} - k_1 - \frac{1}{2}\left(\frac{H}{D}\right)^2k_2 & k_1 + \frac{1}{2}\left(\frac{H}{D}\right)^2k_2 & -\frac{H}{D}k_2 \\ k_1 + \frac{1}{2}\left(\frac{H}{D}\right)^2k_2 & m_1\omega^2 - k_1 - \frac{1}{2}\left(\frac{H}{D}\right)^2k_2 & \frac{H}{D}k_2 \\ -\frac{H}{2D}k_2 & \frac{H}{2D}k_2 & m_2\omega^2 - k_2 \end{bmatrix} \times \begin{Bmatrix} W_0 \\ U_1 \\ U_2 \end{Bmatrix} = 0 \quad (14)$$

To obtain the non-trivial solutions of Eq. (14), the determinant of the coefficient matrix should be set to 0. And the band structure will be obtained to describe the flexural wave propagation of the metamaterial beam.

### 3. Theoretical and numerical results

In order to validate the Hamilton theory presented above, a finite LLR beam consisting of 40 unit cells is calculated in ANSYS 15.0 [21]. BEAM 4 is used to construct the homogeneous beam, and mapped meshing technique is employed to discretise the beam and to assure the results' accuracy. A harmonic force with different frequencies is applied on the left end of the beam. The parameters for a typical unit cell are as follows.

For the homogeneous beam: the unit length  $L = 0.05$  m, the diameter of the cross-section  $R = 0.01$  m, the Young's modulus  $E = 2.1 \times 10^{11}$  Pa, the Poisson ratio  $\nu = 0.3$ , and the mass density  $\rho = 7800$  kg/m<sup>3</sup>.  $F = F_0e^{j\omega t} = 100e^{j\omega t}$  is applied at  $x = 0$  m.

For the vertical resonator: the vertical spring constant  $k_1 = 1 \times 10^5$  N/m, the vertical mass  $m_1 = 0.01$  kg.

For the lateral local resonance:  $m_2 = 0.005$  kg,  $k_2 = 1 \times 10^5$  N/m,  $H = 0.01$  m,  $D = 0.02$  m.

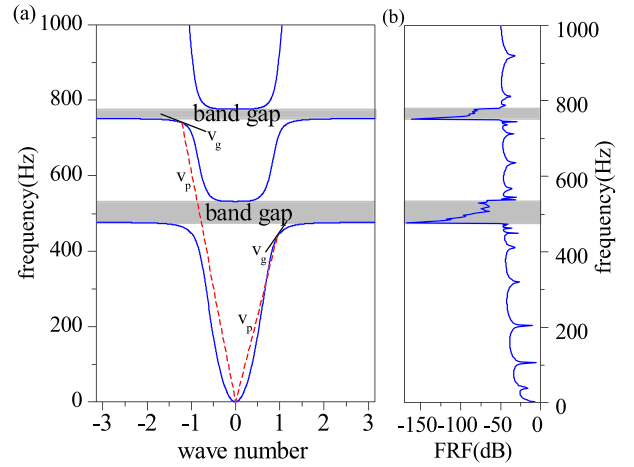


Fig. 2. Theoretical band structures and FRF of a finite sample with 40 unit cells.

The finite element model and FRF matrix can be expressed as

$$\mathbf{M}\{\ddot{q}\} + \mathbf{C}\{\dot{q}\} + \mathbf{K}\{q\} = \{F\} \quad (15a)$$

$$\{F\} = \{0, 0, 0, F_0e^{j\omega t}, 0, \dots\}^T \quad (15b)$$

$$\mathbf{H} = [-\omega^2\mathbf{M} + j\omega\mathbf{C} + \mathbf{K}]^{-1} \quad (15c)$$

$$\{q\} = \mathbf{H}\{F\} \quad (15d)$$

where  $\mathbf{M}$ ,  $\mathbf{C}$  and  $\mathbf{K}$  represent the mass matrix, damping matrix and stiffness matrix of the discretised finite beam model,  $\{q\}$  and  $\{F\}$  denote the displacement and force vector. Eq. (15) is solved using the commercial software ANSYS, and the FRF can be obtained by extracting the dynamic response of the finite beam at the other end. Both the theoretical results of dispersion relation and FRF of a finite metamaterial beam with 40 unit cells are shown in Fig. 2.

From Fig. 2(a), it can be seen that the metamaterial beam can generate two band gaps which are 476–532 Hz and 751–776 Hz, respectively. Correspondingly, in Fig. 2(b), flexural waves within the band gaps are totally blocked. The good consistency of the theoretical results and the FEM results validate the accuracy of each other. From the vibration shape at different frequencies, we found that for the first band gap, it is the vertical resonator that plays the main role whose resonance is 503 Hz, and part of the energy is transformed to the lateral resonators through the four-link-mechanism. While for the second band gap, the flexural energy has been largely transformed to the lateral resonators, which vibrates vigorously to absorb the flexural wave in  $x$  direction. Waves with frequency within both of the band gaps can be efficiently attenuated by the metamaterial beam, which provides a method of multi-flexural vibration control of beams.

In the present study, we utilized the definition of phase velocity and group velocity of a harmonic wave [22]

$$v_p = \frac{\omega}{\beta}, \quad v_g = \frac{d\omega}{d\beta} \quad (16)$$

The phase velocity is obtained by connecting a certain point on the dispersion curve and the origin, while the tangential value of certain point represents the group velocity, as shown in Fig. 2(a). It can be seen that the sign of phase velocity is the same as that of the group velocity, while the magnitudes are not. The wave vector points in the direction of the phase velocity, and the group velocity determines the direction of the acoustic energy in the beam. The absolute value of the phase velocity decreases as wave vector tends to the edge of the Brillouin zone, which means the frequency oscillations are distributed less densely in space. For the group velocity, it goes to zero when the frequency approaches either the

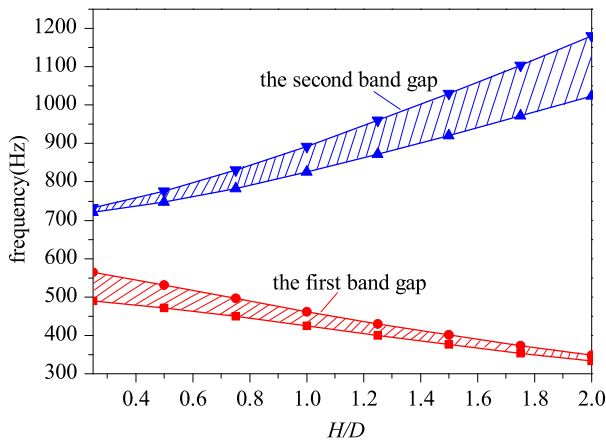


Fig. 3. Effect of  $H/D$  on the band gaps.

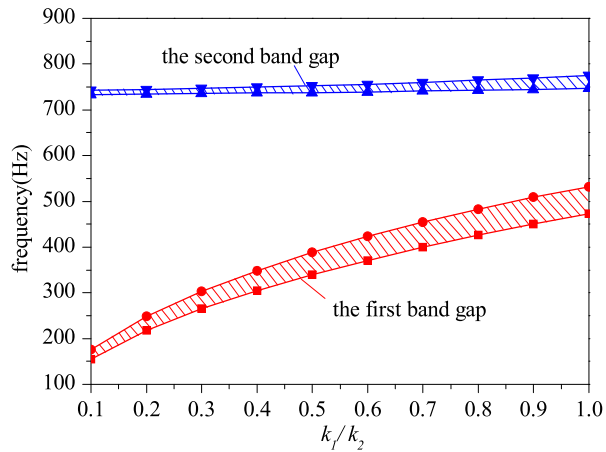


Fig. 4. Effects of the stiffness on the band gaps.

upper edge or the lower edge of the band gaps, which implies that the energy distribution becomes more stationary.

From the analysis, the four-link-mechanism determines the transformation from flexural wave to longitudinal wave. And the influence of the parameter of the four-link-mechanism on the propagation of flexural waves is investigated in Fig. 3. During the calculation, the other parameters are fixed, including those for the beam, the vertical resonator and the lateral resonator.

In Fig. 3, as the ratio of  $H/D$  increases, the first band gap goes to lower frequency range with the gap width decreasing, while the second band gap is broadened to higher frequency range. The trend of the band gaps means that larger ratio of  $H/D$  helps the transformation from flexural wave to longitudinal wave in higher frequency range. And the changes of the position and gap width of the band gaps demonstrate that the four-link mechanism could flexibly tune the band gaps without changing the resonators, which is useful in the field of flexural wave absorption and vibration suppression design.

Another important factor which impacts the band gaps is the stiffness of the springs. The stiffness determines the resonance of the local resonators which induces the band gaps. Therefore, investigation of effects of the stiffness on band gaps is helpful. During the calculation, we assume that  $k_2 = 1 \times 10^5$  N/m, and  $k_1$  is variable with the ratio of  $k_1/k_2$  ranging from 0.1 to 1. The numerical results are demonstrated in Fig. 4.

Since the varying value is the vertical spring's constants, the resonance of the vertical resonator increases along with an increase in the ratio of  $k_1/k_2$ . In Fig. 4, it can be seen that the first band gap shifts to higher frequency range, while the second band

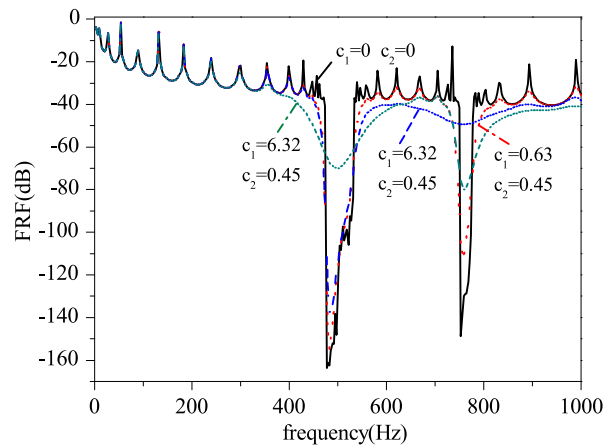


Fig. 5. Effects of damping on the band gaps.

gap remains with the ratio of  $k_1/k_2$  increasing. Meanwhile, the gap width of both the band gaps is slightly broadened. From the trend of the band gaps, it can be concluded that the variation of the stiffness has little influence on the transformation of the waves. However, the corresponding stiffness may modulate the position of the band gaps in different frequency ranges.

From previous knowledge, damping could smooth and lower the response peaks and broaden the band gaps. However, there are two different resonators in this metamaterial beam. The effect of damping from the resonators on the band gaps are investigated numerically and shown in Fig. 5.

In Fig. 5,  $c_1$  denotes the damping from the vertical resonator and  $c_2$  denotes the damping from the LLR substructure. It can be seen that damping has significant influence on the band gaps. When small damping is added to the two resonators, corresponding the comparison of  $c_1 = 0, c_2 = 0$  and  $c_1 = 0.63, c_2 = 0.45$ , the response peaks between the two band gaps and in higher frequency range is lowered slightly. With  $c_1$  increasing while  $c_2$  unchanged, response had been largely attenuated except the much low-frequency range. On the other hand, as  $c_2$  increases while  $c_1$  remains, the second band gap disappears, and the first band gap changes little. In all of these cases, damping could help smooth and lower the response peaks while the band gap effect has been deactivated in different extent. Moreover, damping from the vertical resonator affects both of the two band gaps, while damping from the LLR substructure has little influence on the first band gap.

#### 4. Conclusions

In summary, we have theoretically and numerically investigated the dynamic characteristics of the flexural wave propagation in an Euler–Bernoulli beam with LLR substructures attached. Results show that it can generate two band gaps to stop the flexural wave propagation. The formation mechanism of the two band gaps is owing to the transformation from the flexural wave to longitudinal wave through the four-link-mechanism, which stimulate the lateral resonance to create inertial forces to counterbalance the shear forces of the plate, resulting in wave suppression in the other directions. The transformation, as well as the band gaps, can be flexibly tuned by changing the geometry parameter of the LLR substructure. Phase velocity and group velocity are analysed to demonstrate phase variation and energy propagation in space. Finite element results show flexural waves can be efficiently blocked within the band gaps and damping from the resonators may broaden the band gaps and help smooth and lower the response peaks at the sacrifice of the band gap effect. The study conducted in this paper is promising in the flexural absorber and isolator design for vibration and noise control.

## Acknowledgement

The first author is grateful for the sponsorship from the China Scholarship Council.

## References

- [1] Z. Liu, X. Zhang, Y. Mao, Y.Y. Zhu, Z. Yang, C.T. Chan, P. Sheng, *Science* 289 (2000) 1734.
- [2] P. Sheng, X.X. Zhang, Z. Liu, C.T. Chan, *Physica B, Condens. Matter* 338 (2003) 201.
- [3] X. Wang, *Int. J. Solids Struct.* 51 (2014) 1534.
- [4] T. Wang, M.P. Sheng, H. Wang, Q.H. Qin, *Acoust. Aust.* (2015), <http://dx.doi.org/10.1007/s40857-015-0031-6>.
- [5] H.H. Huang, C.T. Sun, G.L. Huang, *Int. J. Eng. Sci.* 47 (2009) 610.
- [6] S.A. Pope, S. Daley, *Phys. Lett.* 374 (2010) 4250.
- [7] Y. Shanshan, Z. Xiaoming, H. Gengkai, *New J. Phys.* 10 (2008) 043020.
- [8] P.F. Pai, *J. Intell. Mater. Syst. Struct.* 21 (2010) 517.
- [9] G. Wang, J. Wen, X. Wen, *Phys. Rev. B* 71 (2005) 104302.
- [10] J. Chen, C. Sun, *J. Sandw. Struct. Mater.* 13 (2011) 391.
- [11] J. Chen, B. Sharma, C. Sun, *Compos. Struct.* 93 (2011) 2120.
- [12] D. Yu, Y. Liu, G. Wang, L. Cai, J. Qiu, *Phys. Lett.* 348 (2006) 410.
- [13] D. Yu, Y. Liu, G. Wang, H. Zhao, J. Qiu, *J. Appl. Phys.* 100 (2006) 124901.
- [14] Y. Liu, D. Yu, L. Li, H. Zhao, J. Wen, X. Wen, *Phys. Lett.* 362 (2007) 344.
- [15] H. Sun, X. Du, P.F. Pai, *J. Intell. Mater. Syst. Struct.* 21 (2010) 1085.
- [16] Q. Wen, S. Zuo, H. Wei, *Acta Phys. Sin.* 61 (2012) 034301.
- [17] Z. Wang, P. Zhang, Y. Zhang, *Math. Probl. Eng.* 2013 (2013) 1.
- [18] P.F. Pai, H. Peng, S. Jiang, *Int. J. Mech. Sci.* 79 (2014) 195.
- [19] H.H. Huang, C.T. Sun, *J. Mech. Phys. Solids* 59 (2011) 2070.
- [20] Ç. Demir, Ö. Civalek, *Appl. Math. Model.* 37 (2013).
- [21] H.H. Lee, *Finite Element Simulations with ANSYS Workbench 15: Theory, Applications, Case Studies*, Schroff Development Corporation, 2014.
- [22] L. Brillouin, *Wave Propagation and Group Velocity*, Academic Press, 2013.